Molecular Catalysis 514 (2021) 111848

Contents lists available at ScienceDirect

Molecular Catalysis

journal homepage: www.journals.elsevier.com/molecular-catalysis

Kinetics of phosphotungstic acid-catalyzed condensation of levulinic acid with phenol to diphenolic acid: Temperature-controlled regioselectivity

Mohammad Shahinur Rahaman [a], Sarttrawut Tulaphol [b], Md Anwar Hossain [a], Clint N. Evrard [c], Lee M. Thompson [c,*], Noppadon Sathitsuksanoh [a,*]

[a] Department of Chemical Engineering, University of Louisville, Louisville, KY 40292, USA
[b] Sustainable Polymer & Innovative Composite Materials Research Group, Department of Chemistry, Faculty of Science, King Mongkut's University of Technology Thonburi, Bangkok 10140, Thailand
[c] Department of Chemistry, University of Louisville, Louisville, KY 40292, USA

ARTICLE INFO

Keywords:
Phosphotungstic acid
Levulinic acid
Diphenolic acid
Condensation
Regioselectivity
Reaction kinetics

ABSTRACT

Diphenolic acid (DPA) is a renewable compound to produce polycarbonates and epoxy resins. Diphenolic acid is produced by acid-catalyzed condensation of levulinic acid with phenol to form monophenolic acid. Subsequently, monophenolic acid undergoes condensation with phenol to form two DPA isomers, ortho-diphenolic acid (*o,p′*-DPA) and para-diphenolic acid (*p,p′*-DPA). Here we describe a kinetic analysis of solvent-free levulinic acid-phenol condensation catalyzed by phosphotungstic acid at temperatures between 70 and 140°C. The reaction appeared to be pseudo-first-order with respect to levulinic acid when the levulinic acid:phenol molar ratio was four or higher. We determined the kinetic parameters (reaction rate constants, pre-exponential factors, and activation energies) by fitting experimental results to simulated data. Although the activation energies of *o,p′*-DPA, and *p,p′*-DPA formation were higher than their corresponding reverse reactions, the kinetic analyses revealed that a steric effect controls the reaction products. Our findings demonstrated a simple temperature-controlled strategy to achieve a *p,p′*:*o,p′* DPA molar ratio of 28.3 with 87% conversion and 98% selectivity to total DPA. This work provides a potential production route for *p,p′*-DPA from biomass.

1. . Introduction

Negative consequences of processing petroleum feedstock, especially greenhouse gas emissions [1], price volatility [2], and non-renewability [3], have stimulated the search for renewable feedstocks. Plant biomass is renewable, abundant, and cost-effective and can be transformed into platform chemicals, such as 5-hydroxymethylfurfural, levulinic acid, γ-valerolactone, lactic acid, and diphenolic acid [4-8]. Diphenolic acid (DPA) and its derivatives [8-20] are potential renewable alternatives for toxic bisphenol A (2,2-Bis(4-hydroxyphenyl)propane, commonly known as BPA) in water bottles, containers, and dental composites/sealants [8,9,21,22]. Exposure to bisphenol A can cause infertility [23], male impotence [24], heart disease [25], and breast and prostate cancer [26].

Synthesis of DPA involves an acid-catalyzed condensation reaction between phenol and levulinic acid (Scheme 1) [27], which can be obtained from lignin [28] and cellulose [29-31], respectively. The condensation of levulinic acid with phenol forms two DPA isomers, ortho-diphenolic acid (*o,p′*-DPA) and para-diphenolic acid (*p,p′*-DPA). The *p,p′*-DPA isomer is especially desirable in the production of polycarbonate and epoxy grade resins [32]. However, a costly process is required to separate the *o,p′*-isomer from *p,p′*-isomer, which adds to the production cost of plastics. Hence, many investigators have focused on improving regioselectivity to *p,p′*-DPA [33]. Homogenous Brønsted acid catalysts, such as H_2SO_4 and HCl, catalyze condensation between levulinic acid and phenol [34-36]. However, these mineral acids are corrosive, and their residuals from waste streams are expensive to treat [35]. The addition of thiols as an additive improved the *p,p′*:*o,p′*-DPA molar ratio [37,38], but thiol addition in the reaction complicates downstream product purification.

Polyoxometalates (POMs) are versatile catalysts because of their many active sites [39,40]. The Keggin anion family of POMs is expressed as $[XM_{12}O_{40}]^{n-}$ anions, where X = Si and P, M = Mo and W. The Keggin-type POMs with protons as the only countercations are called heteropolyacids (HPAs), such as phosphotungstic acid, silicotungstic acid, silicomolybdic acid, phosphomolybdic acid. These HPAs have high acid strength and less corrosive characteristics compared

* Corresponding authors.
E-mail addresses: lee.thompson.1@louisville.edu (L.M. Thompson), n.sathitsuksanoh@louisville.edu (N. Sathitsuksanoh).

https://doi.org/10.1016/j.mcat.2021.111848
Received 13 February 2021; Received in revised form 18 August 2021; Accepted 20 August 2021
Available online 9 September 2021

with ordinary mineral acids (HBr, H_2SO_4, HNO_3, and HCl) [41,42]. Thus, HPAs have been used widely to catalyze biomass conversion reactions [43,44]. However, HPAs are soluble in water and many organic solvents. Thus, they are difficult to recycle and their presence complicates product purification. Previous studies showed that the HPAs and partly substituted HPAs exhibited high catalytic activity and selectivity to total DPA. However, their regioselectivity to *p,p′*-DPA (<7.3) [45-47] was lower than the regioselectivity obtained by addition of thiol and Brønsted acid ionic liquid additives [34,37,38]. Moreover, a detailed kinetic analysis of this reaction catalyzed by HPAs have not been assessed, thereby limiting our understanding of how to control the regioselectivity of DPA formation.

Here, we evaluated the catalytic performance of selected heteropolyacids on the condensation of levulinic acid with phenol, and we detailed the kinetics of this reaction. We demonstrated that phosphotungstic acid was the most selective to *p,p′*-DPA. Then we determined the effect of the reaction temperature on the regioselectivity to *p,p′*-DPA catalyzed by phosphotungstic acid. Reaction temperature regulated the regioselectivity to *p,p′*-DPA with 28.3 *p,p′*:*o,p′*-DPA molar ratio at 87% conversion at 140°C. Then we developed the kinetic analysis of this reaction to reveal the reaction mechanism and understand how to control the regioselectivity of DPA formation.

2. Materials and methods

2.1. Materials

All chemicals were analytical grade and used without further purification unless noted. Levulinic acid (98%, Sigma-Aldrich, St. Louis, MO, USA), phenol (VWR International, Radnor, PA, USA), and hexadecane (99%, Alfa Aesar, Haverhill, MA, USA), were used as received. The catalysts, phosphotungstic acid (99%, Strem Chemicals, Newburyport, MA, USA), silicotungstic acid hydrate (Electron microscopy sciences, Hatfield, PA, USA)), silicomolybdic acid (72.72% MoO_3, Strem Chemicals, Newburyport, MA, USA), phosphomolybdic acid hydrate (Alfa Aesar, Haverhill, MA, USA) were purchased and used as received.

2.2. Condensation reaction between levulinic acid and phenol

The condensation reaction between levulinic acid and phenol was performed in a 15 mL glass pressure tube (Ace Glass Inc., USA). Typically, a 1:4 molar ratio mixture of levulinic acid (0.64 mmol) and phenol (2.54 mmol, ~0.2mL) was added to the pressure tube. Then, 1 mol % catalyst with respect to levulinic acid was used in all experiments, unless otherwise noted. Hexadecane was added as an internal standard for the quantification of levulinic acid conversion and product yields. After loading the catalyst into the tube, it was sealed and placed in an oil bath at temperatures of 70 - 140°C. The tube was equilibrated for 5 min to the desired temperature before proceeding with the reaction. Preliminary experiments were performed at stirring speeds between 300 and 900 rpm. No difference in reaction conversion was observed at different stirring speeds. Thus, mass transfer limitation was negligible within this interval of stirring speed, and we used a rotating speed of 600 rpm for all experiments. The reaction products were withdrawn over time to measure the concentration of reactants and products. The reaction was immediately stopped by quenching in an ice bath. Ethyl acetate was added to dissolve unreacted reactants and reaction products prior to analysis by Gas Chromatography (GC). All experiments were performed in triplicate, and the standard deviation of reaction products was less than 8 %.

2.3. Product analysis

Unreacted reactants, intermediates, and reaction products in the samples were separated and quantified by GC. The reaction products were silylated to improve volatility, thermal stability, separation, resolution, and response by GC analysis [48,49]. The silylation procedure was reported elsewhere [50-52] with a slight modification. In short, the samples (~200 μL) were mixed with 200 μL N,O-bis(trimethylsilyl) trifluoroacetamide (BSTFA) as a silylating agent and 10% trimethylchlorosilane (TMCS) as a silylating catalyst. The silylation took place at 70°C for 1h to allow the active hydrogens of the compounds in the reaction products to be replaced by an alkylsilyl group, creating silyl derivatives that were more volatile, less polar, and more thermally stable compared with silylated reaction products [53]. The silylated sample was analyzed by Gas Chromatography (7890B GC) (Agilent Technologies, Santa Clara, CA, USA) equipped with Mass spectrometry (MS) and Flame Ionization Detector (FID). The reactants and reaction products were separated using an HP-5MS column (30mx0.25mmx0.25μm, Agilent Technologies, Santa Clara, CA, USA). Levulinic acid conversion and yields of DPA were calculated as follows:

$$\text{Conversion of levulinic acid (\%)} = \frac{\text{levulinic acid converted (mol)}}{\text{levulinic acid initial (mol)}} \times 100$$

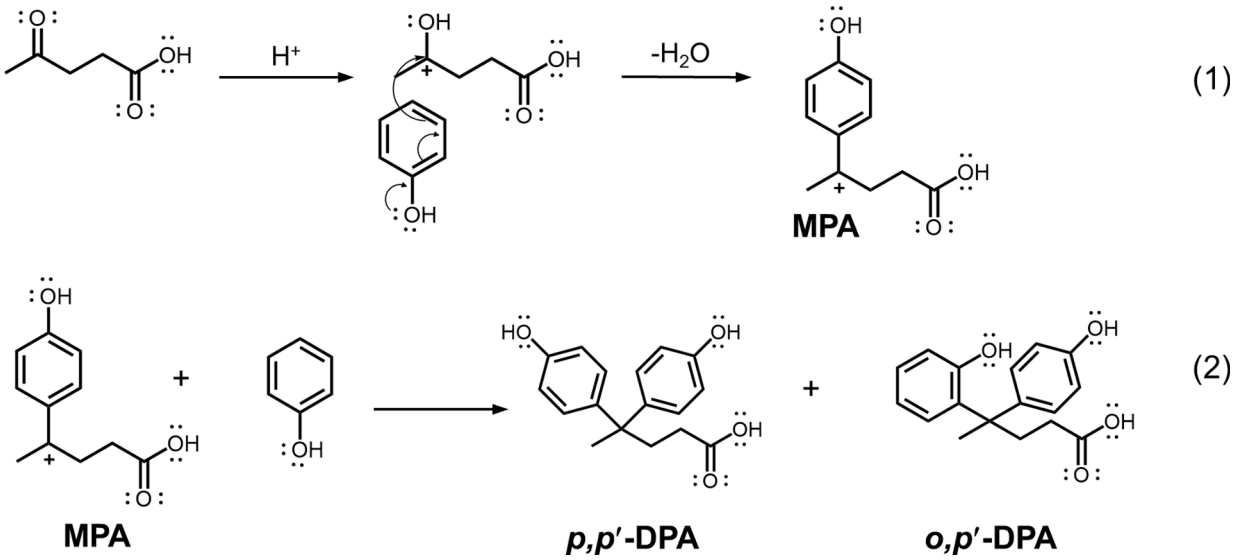

Scheme 1. Proposed reaction mechanism of the condensation of levulinic acid-phenol to produce *o,p′*- and *p,p′*-DPA.

$$\text{Yield of products (\%)} = \frac{\text{product generated (mol)}}{\text{levulinic acid initial (mol)}} \times 100$$

The mass balance of reactants and products showed less than 7% standard deviation unless otherwise noted. The specific activity (rate of the reacted levulinic acid per mol of catalyst) and productivity (rate of the desired product formation per mol of catalyst) were indicators of the rate at which the catalyst was able to convert reactant and produce the desired product, respectively. The two parameters were defined as follows:

$$\text{Specific activity } (h^{-1}) = \frac{\text{levulinic acid reacted (mol)}}{\text{catalyst (mol) x time (h)}}$$

$$\text{Productivity } (h^{-1}) = \frac{\text{total diphenolic acid generated (mol)}}{\text{catalyst (mol) x time (h)}}$$

One mole of heteropolyacid was assumed to give one mole of the acid sites (active proton). Protons of heteropolyacids in a polar solvent (ethanol) dissociate, leaving only one active proton [54,55]. Hence, heteropolyacids behave like monoprotic acids. Phenol acted as both reactant and solvent.

2.4. Determination of kinetic rate constants and activation energies

The experimental results were fit to a rate expression that included the concentrations of levulinic acid (LA), mono-phenolic acid (MPA), ortho-diphenolic acid (*o,p′*-DPA), and para-diphenolic acid (*p,p′*-DPA). The levulinic acid:phenol molar ratio was varied from 1:2 (stoichiometric ratio) to 1:4, 1:6, and 1:10 to determine the molar ratio that provided excess phenol. A levulinic acid:phenol molar ratio higher than 1:4 resulted in constant levulinic acid conversion and yield of total diphenolic acid (DPA), which suggested a pseudo first-order reaction with respect to levulinic acid (Fig. S1). For this reason, the levulinic acid: phenol molar ratio of 1:4 was used for the reaction throughout this study. The Excel solver was used to estimate the reaction rate constants (k) with the Generalized Reduced Gradient (GRG) nonlinear solving method. Nonlinear least-square regression analysis was used to calculate the difference between the experimental data and the estimated values by changing the reaction rate constants. Various initial guesses were used for estimation to ensure that the estimated kinetic parameters converged to the same minimum. The best fit was defined as the estimated kinetic values that gave a minimal difference. The fitting was conducted for various reaction temperatures simultaneously using a single set of initial kinetic parameters to find the fit for the rate expression.

3. Results

To understand how to control the regioselectivity to *p,p′*-diphenolic acid (*p,p′*-DPA) in the condensation of levulinic acid-phenol, we first screened four Keggin-type heteropolyacids. Next, we selected the best-performing acid catalyst for this condensation reaction and determined the effect of temperature on the catalytic activity and selectivity to *p,p′*-DPA. Then, we determined the kinetic parameters to understand how they affected the regioselectivity of DPA.

3.1. Initial catalyst screening for condensation of levulinic acid and phenol

Initially, to evaluate the catalytic performance of selected Keggin-type heteropolyacids and mineral acids for condensation of levulinic acid with phenol, we measured the catalysts specific activities (rate of the reacted levulinic acid per mol of catalyst) and productivity (rate of the DPA formation per mol of catalyst) (Table 1). As a control, no conversion of levulinic acid occurred in the absence of catalysts, which suggested that this reaction was not catalyzed by the carboxylic acid group of levulinic acid. All catalysts were active in the condensation of levulinic acid with phenol as shown by high catalyst specific activity (6.5-16.7 h^{-1}). We observed *p,p′*-DPA and *o,p′*-DPA as main reaction products; a small amount of monophenolic acid (MPA) was detected, which suggested that monophenolic acid was an intermediate in the reaction. We found that phosphotungstic acid had high specific activity of 9.2 h^{-1} and the highest productivity of 7.7 h^{-1} (entry 1) compared with other catalysts at 100°C after 6 h. Although other heteropolyacids, such as silicotungstic acid, silicomolybdic acid, and phosphomolybdic acid, were active in levulinic acid conversion with high specific activities of 11 – 13 h^{-1}, they were less selective to DPA formation (entries 2-4). Their productivities were 0.0 - 4.1 h^{-1}, lower than that of phosphotungstic acid (7.7 h^{-1}). Sulfuric acid and hydrochloric acid were active in levulinic acid conversion, but they were not selective to DPA, as shown in low productivity (entries 5 and 6). Because of the high specific activity and productivity, we chose phosphotungstic acid for further studies.

Table 1
Condensation of levulinic acid with phenol by selected acid catalysts

Entry	Catalyst	Specific activity[a] (h^{-1})	Productivity[b] (h^{-1})
1	Phosphotungstic acid ($H_3PW_{12}O_{40}$)	9.2	7.7
2	Silicotungstic acid ($H_4SiW_{12}O_{40}$)	11.5	4.1
3	Silicomolybdic acid ($H_4SiMo_{12}O_{40}$)	13.1	2.8
4	Phosphomolybdic acid ($H_3PMo_{12}O_{40}$)	12.9	nd[c]
5	Hydrochloric acid (HCl)	6.5	1.0
6	Sulfuric acid (H_2SO_4)	16.7	0.0
7	No cat	-	nd[c]

Reaction condition: 1 mol% catalyst (with respect to levulinic acid) at 1:4 molar ratio of levulinic acid: phenol at 100°C for 6 h.
[a] specific activity is defined as mol of levulinic acid reacted per mol of catalyst per time
[b] productivity is defined as mol of total DPA (*p,p′*-DPA and *o,p′*-DPA) generated per mol of catalyst per time
[c] not detectable. The concentration of the DPA was lower than the detection limit of the detector

Next, to investigate the effect of phosphotungstic acid loading on catalytic performance, we performed condensation of levulinic acid with phenol using 0.5, 1.0, and 5.0 mol% catalyst (with respect to the levulinic acid) at 100°C for 6h (Fig. S2). An increase in catalyst loading increased the rate of levulinic acid conversion. However, increased catalyst loading did not affect the selectivity to *p,p′*-DPA and *o,p′*-DPA. Our findings agreed with results of Yu et al. who showed that increasing the loading of Cs-substituted Wells-Dawson type heteropolyacids did not affect the selectivity to *p,p′*-DPA [45]. To detail the mechanism of condensation of levulinic acid with phenol, we needed to evaluate the catalytic performance at a low conversion to minimize the effect of side reactions. For these reasons, we used 1.0 mol% catalyst loading for the remainder of the studies.

3.2. Effect of reaction temperature on the condensation of levulinic acid with phenol

To investigate the effect of reaction temperature on levulinic acid-phenol condensation catalyzed by phosphotungstic acid, we performed the condensation reaction at temperatures between 70 and 140°C. In all experiments, the sum of unreacted levulinic acid, monophenolic acid (MPA), and total diphenolic acid was close to the initial mol of levulinic acid, which suggested that there was minimal decomposition of levulinic acid, intermediates, and products. An increase in reaction temperature promoted the levulinic acid conversion and total DPA yield. We observed *p,p′*-DPA and *o,p′*-DPA as main reaction products. The conversion rate of

levulinic acid and selectivity to total DPA progressively increased over time (Fig. 1A and B). We also detected a small concentration of MPA in the reaction. The selectivity profile of MPA was volcano-shaped (Fig. 1C), which indicated that MPA was the intermediate. Increasing reaction temperature from 70 to 140°C decreased the MPA selectivity and increased the *p,p′*-DPA selectivity (Fig. S3). The formation of *p,p′*-DPA was more favorable than *o,p′*-DPA in all cases as shown in *p,p′: o,p′* molar ratio >1 (Fig. 1D), in agreement with previous studies which showed *p,p′: o,p′* molar ratio >1 by Brønsted acidic catalysts [33,46,56,57]. Interestingly, an increase in reaction temperature also enhanced the *p,p′: o,p′* molar ratio, which suggested that regioselectivity of DPA isomer depended strongly on the reaction temperature. Reaction temperatures below 100°C provided a low regioselectivity to *p,p′*-DPA (low *p,p′*: *o,p′* molar ratio <10). Reaction temperatures higher than 120 °C drastically improved the *p,p′*: *o,p′* molar ratio, which reached 28.3. Together, these results suggested that reaction temperature controlled catalytic activity and regioselectivity of DPA.

3.3. Kinetic parameters of the condensation of levulinic acid with phenol

Next, we determined the kinetic parameters of the condensation reaction to understand the behavior of the intermediates and products and the effect of reaction temperature on regioselectivity. Scheme 1 shows the commonly accepted mechanism of levulinic acid condensation with phenol [47]. The condensation reaction begins by protonation of the ketone group of levulinic acid and subsequent electrophilic attack of phenol, forming reactive carbonium ion monophenolic acid (MPA) [33,58]. This MPA attacks the second molecule of phenol to form *o,p′*-DPA (*o,p′*-DPA formation) or *p,p′*-DPA (*p,p′*-DPA formation). The *o,p′*-DPA can isomerize into *p,p′*-DPA by bond cleavage between phenol and the bridging carbon atom in the reverse direction of the electrophilic aromatic substitution by protonation of the aromatic ring [59] to form the monophenolic acid. Then the resulting monophenolic acid attacks a molecule of phenol to form *p,p′*-DPA.

To understand the kinetic behavior, we proposed the chemical pathway (Scheme 2) that involves MPA formation (Step 1), followed by *o,p′*-DPA formation (Step 2) or *p,p′*-DPA formation (Step 3). The rate expressions of three reaction steps are expressed and fit with experimental data (see Supplementary Information).

The simulated curves fit well with experimental data (Fig. 2). Then, we determined the reaction rate (k) constants based on the proposed mechanism in Scheme 1 (Table S1). The resulting k increased with increasing reaction temperature (Fig. 3). With increasing temperature, we observed a significant increase in the reaction rate constant k_{1r} (MPA conversion to levulinic acid and phenol), k_{2f} (MPA condensation to *o,p′*-DPA), and k_{3f} (MPA condensation to *p,p′*-DPA). Furthermore, k_{1r}, k_{2f}, and k_{3f} values were higher than k_{1f}, k_{2r}, and k_3, respectively. These results confirmed that the MPA was a reactive intermediate, in agreement with the low MPA concentration detected in the reaction.

The temperature dependence of the resulting k values demonstrated Arrhenius behavior (Fig. 3A-C). The gap between forward and reverse lines at a specific temperature for each k implies the relative reaction rates between forward and reverse reactions. For Step 1, k_{1r} was higher than k_{1f}, which indicated that MPA intermediate was not able to form in any significant concentration. For example, Steps 1 and 3 showed that the reaction away from MPA was much faster than towards it. The gap between forward and reverse lines remained relatively constant as a function of temperature, which suggested that the relative reaction rates of Step 1 remained constant. For Step 2, the forward and reverse rate constants are close across all temperatures. Like for Step 1, the constant difference suggested that the relative reaction rates of Step 2 were temperature independent. For Step 3, the rate of *p,p′*-DPA formation was higher than that of *p,p′*-DPA decomposition as a function of temperature. Interestingly, the gap between forward and reverse lines became significantly larger as reaction temperature increased. These results suggested that (1) the *p,p′*-DPA formation was sensitive to changes in reaction temperature, and (2) high reaction temperature shifted equilibrium to the *p,p′*-DPA formation.

On the basis of these Arrhenius behaviors, we calculated the corresponding activation energies and pre-exponential factors (Table 2). Interestingly, the high activation energy of forward reactions, MPA formation ($E_{a,1f}$), *o,p′*-DPA formation ($E_{a,2f}$) formation, and *p,p′*-DPA formation ($E_{a,3f}$), suggested that these formation steps were more sensitive to temperature than the reverse reactions (Fig. 3B and C). However, the higher activation energy of the forward reactions would suggest that forward reaction rate constants are smaller than reverse reaction rate constants, which is not the case as illustrated in Fig. 3C. Furthermore, we should observe low DPA yield/selectivity, which contradicts our experimental findings that showed a high DPA selectivity as the reaction proceeded.

Although many investigators who have studied the kinetics of biomass conversion pathways discuss reactions in terms of activation energies, the steric (entropic) effect cannot be ruled out because this effect is important to some reactions that involve bulky molecules (e.g., DPA) [60]. To understand the mechanism of this condensation of levulinic acid-phenol, we further evaluated the pre-exponential factors. From collision theory, the pre-exponential factor is a measure of the rate at which collision of the reactive molecules occurs and is a proxy for

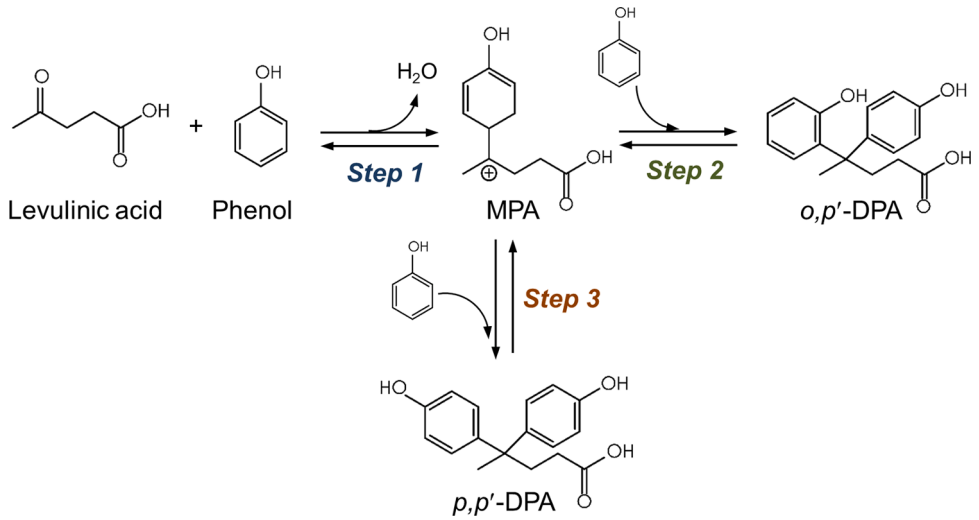

Scheme 2. Chemical pathways for the kinetic analyses of condensation of levulinic acid and phenol.

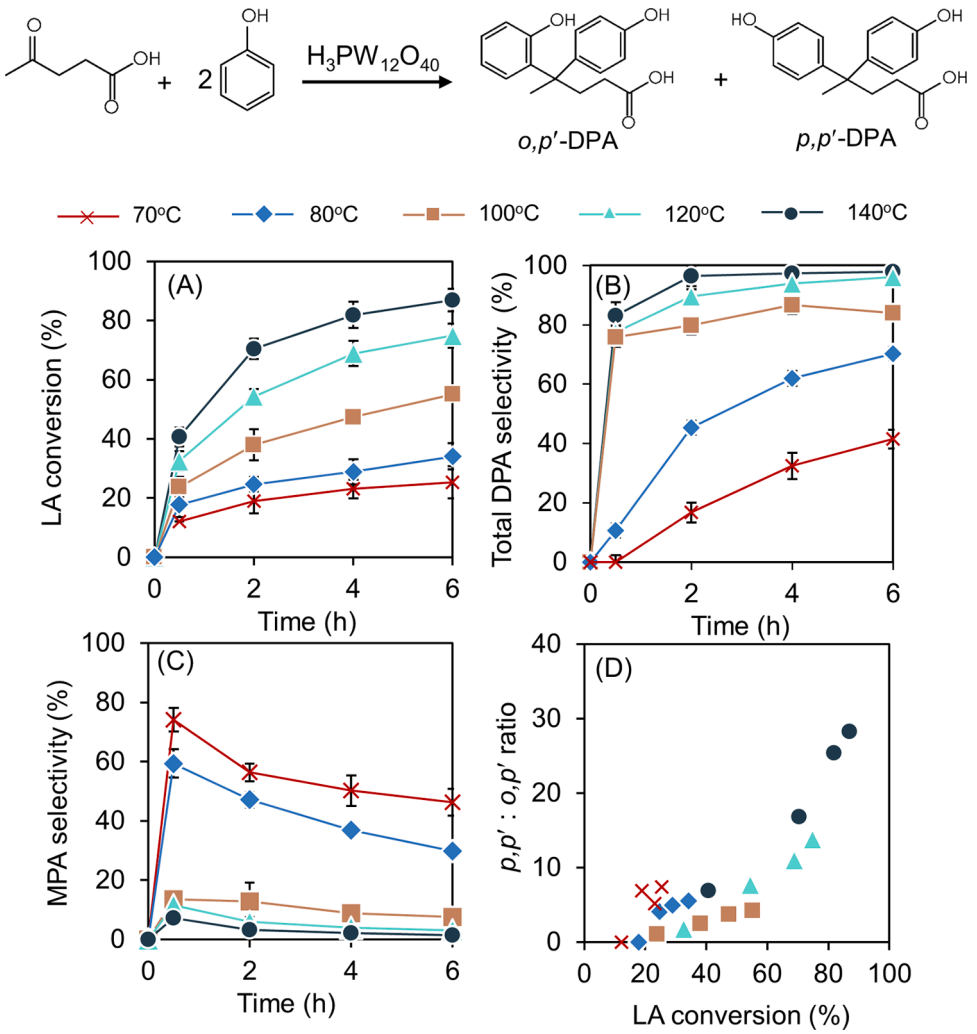

Fig. 1. Evolution of levulinic acid conversion (A), total DPA selectivity (B) and monophenolic acid (MPA) selectivity (C). The *p,p′*-DPA: *o,p′*-DPA ratio as a function of levulinic acid conversion (D). Reaction conditions: molar ratio of levulinic acid:phenol = 1: 4, phosphotungstic acid loading = 1 mol%.

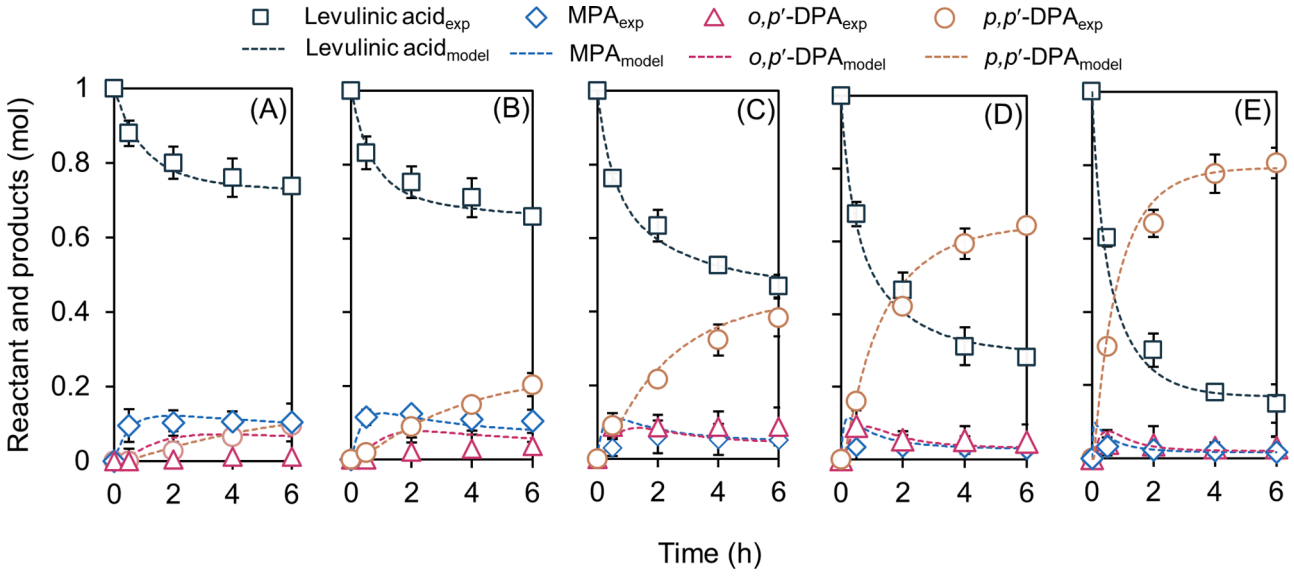

Fig. 2. Fitted curves of simulated and experimental data at (A) 70 °C; (B) 80 °C; (C) 100 °C; (D) 120 °C and (E) 140 °C. Reaction conditions: molar ratio of levulinic acid: phenol = 1:4, 1 mol % phosphotungstic acid loading. The dashed line and dots represent simulated and experimental data, respectively.

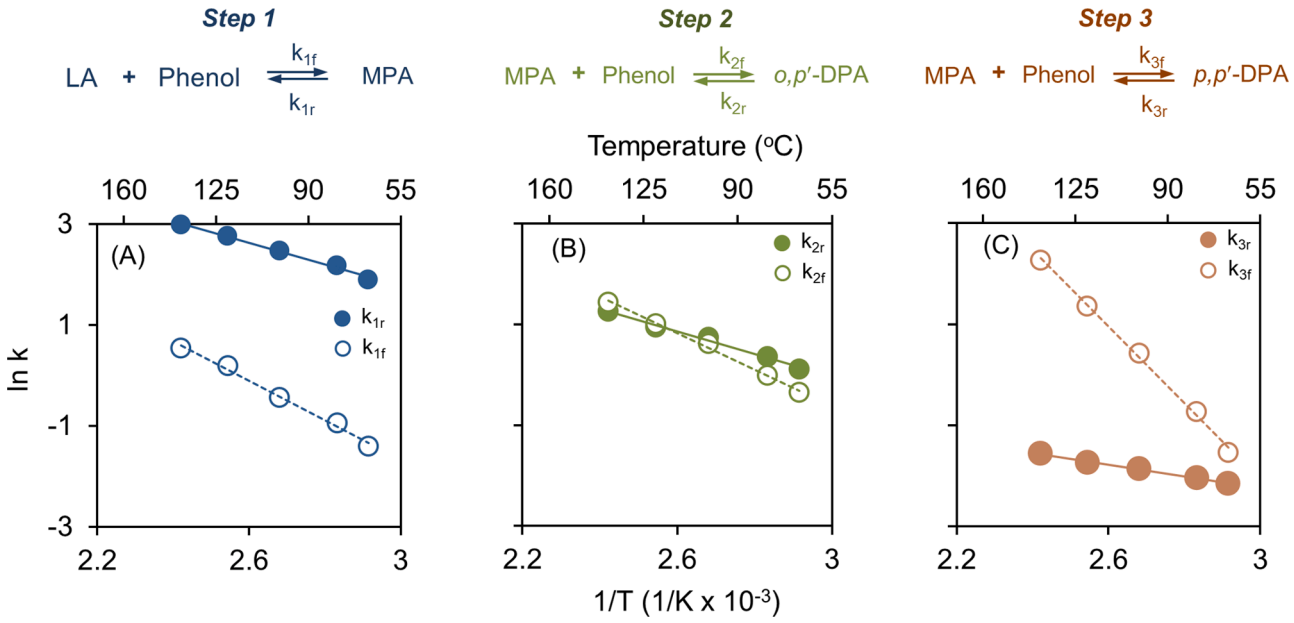

Fig. 3. Relationship between reaction rate constant (k_i) with inverse temperature of the monophenolic acid (MPA) formation from condensation of levulinic acid (LA) and phenol (A), *o,p′*-DPA formation from the second condensation of MPA and phenol (B), and *p,p′*-DPA formation from the second condensation of MPA and phenol (C).

Table 2
Kinetic parameters obtained from fitting the experimental data with the kinetic model at various temperatures.

Parameter	Reaction rate constant					
	k_{1f}	k_{1r}	k_{2f}	k_{2r}	k_{3f}	k_{3r}
E_a (kj. mol^{-1})	32.63	17.53	24.04	14.86	62.99	9.62
A (s^{-1})	8.22	8.89×10^{-1}	7.53	2.48×10^{-1}	2.58×10^{5}	9.47×10^{-4}
R^2	0.97	0.99	0.98	0.99	0.99	0.99

steric effects in the reaction [61]. The calculated pre-exponential factors of all forward reactions were significantly higher compared with reverse reactions, which suggested a higher collision frequency and/or a smaller steric factor [62]. In particular, the pre-exponential factor of the *p,p′*-DPA formation (A_{3f}, 2.58×10^5 s^{-1}) was five orders of magnitude higher than that of *o,p′*-DPA formation (A_{2f}, 7.53 s^{-1}), which can be ascribed to a lower orientational dependence of the activated complex leading to formation of *p,p′*-DPA, and fits with the experimental findings in which *p,p′*-DPA was formed preferentially compared to *o,p′*-DPA. The pre-exponential factor of *p,p′*-DPA formation in the forward direction (A_{3f}) was eight orders of magnitude higher than the pre-exponential factor of the reverse direction (A_{3r}, 9.47×10^{-4} s^{-1}). In sum, these results suggested that steric effects control the observed reactivity.

4. Discussion

In this study, we described the effect of reaction temperature on the regioselectivity of *p,p′*-DPA formation catalyzed by Keggin-type heteropolyacids. Among the Keggin-type heteropolyacids that we tested, phosphotungstic acid was the most selective to total DPA with 98% DPA selectivity at 87% conversion of levulinic acid. Also, the resulting kinetic parameters suggested that the steric effect controls levulinic acid-phenol condensation and regioselectivity to *p,p′*-DPA.

The ability to control regioselectivity by temperature was a significant finding. The *p,p′*-DPA is preferentially formed in the condensation of levulinic acid-phenol with the *p,p′: o,p′*-DPA ratio >1 by acid catalysts, such as heteropolyacids [63], mineral acids (HCl) [47], zeolites [45], and sulfonated hyperbranched poly(arylene oxindole)s [33,56] (Table S2). However, results of most investigations of the DPA production by acid catalysts showed low *p,p′: o,p′*-DPA molar ratios of 1.1 – 8.7 [27,37,63,64]. For example, Guo et al. used supported phosphotungstic acid on SiO_2 particles for the condensation of levulinic acid with phenol at 100°C for 8 h with a phenol: levulinic acid ratio of 4 [47]. Their *p,p′: o,p′*-DPA molar ratio was ~2.1-3.6 on all supported phosphotungstic acid. Yu et al. used Cs-substituted Wells-Dawson type heteropolyacids, $CsH_{6-x}P_2W_{18}O_{62}$ (x=1.5-6.0) to reach the *p,p′: o,p′*-DPA ratio of 7.3 [45]. To advance the *p,p′: o,p′*-DPA ratio to greater than 10, Van de Vyver et al. used additives. Their synthesized sulfonated hyperbranched poly(arylene oxindole)s acid catalysts showed the *p,p′: o,p′*-DPA ratio of 7.6. With a thiol additive (ethanethiol), the side chain of the thiol introduced steric hindrance and boosted the *p,p′: o,p′*-DPA molar ratio to ~40 at 23 % levulinic acid conversion [33,37]. Liu et al. used a combination of Bronsted acid ionic liquids as a catalyst and additive to promote the *p,p′: o,p′*-DPA molar ratio over 100 [65]. However, additives complicate product separation during downstream processing. An increase in reaction temperature from 70 to 140°C increased *p,p′: o,p′* molar ratio from 7.4 to 28.3. This temperature increase shifted the equilibrium to formation *p,p′*-DPA formation preferentially as evidenced by increased equilibrium constant of *p,p′*-DPA and *o,p′*-DPA formation steps by 25 and 2 times, respectively. Our findings suggested that the steric effect controls the mechanism of this condensation of levulinic acid-phenol, in agreement with a report by Van de Vyver et al.[56]. Elevated reaction temperature introduces steric hindrance and shifts the regioselectivity to *p,p′*-DPA.

The identification of steric control of the levulinic acid-phenol condensation products is another important finding. The calculated activation energy of all forward reactions was higher than the activation energy of reverse reactions, which implied that the formation of MPA, *o,p′*-DPA, and *p,p′*-DPA was unfavorable and contrary to our experimental results. However, the pre-exponential factor of forward reactions was higher than that of reverse reaction; particularly, the pre-exponential factor of the *p,p′*-DPA formation was several orders of magnitude higher than that of its reverse reaction and *o,p′*-DPA formation. These results suggested that the collision of reactive molecules to form *p,p′*-DPA occurred with greater frequency or was less dependent on the orientation of reacting molecules, compared with formation of the *o,p′*-DPA and the

decomposition of *p,p′*-DPA. Moreover, this high pre-exponential factor of *p,p′*-DPA formation suggested that the steric effect controls the reaction products and explains the observed *p,p′: o,p′*-DPA ratio >1.0.

This work not only explains the kinetics and mechanism of the condensation of levulinic acid-phenol, but also provides an additive-free catalytic strategy to promote the regioselectivity to *p,p′*-DPA. Although this catalytic system is effective at *p,p′*-DPA formation, there are two limitations, namely, the use of homogeneous catalysts and high temperature. Further studies will focus on the development of supported phosphotungstic acid catalysts and their recyclability and explain the tradeoff between high-temperature operation and high regioselectivity to *p,p′*-DPA.

5. Conclusion

Detailed knowledge of the kinetic parameters of condensation of levulinic acid-phenol enhances our understanding of the reaction mechanism and provides a strategy to improve the regioselectivity toward *p,p′*-DPA. Our results demonstrated that increasing reaction temperature in phosphotungstic acid-catalyzed condensation of levulinic acid with phenol not only accelerated the condensation rate but also it shifted the regioselectivity toward the desired *p,p′*-DPA. Our kinetic analyses revealed a steric effect controls the reactivity, and *o,p′*- and *p,p′*-DPA formations occur readily. This knowledge will aid in the development of recyclable catalysts to maximize the regioselectivity to *p,p′*-DPA.

CRediT authorship contribution statement

Mohammad Shahinur Rahaman: Conceptualization, Methodology, Investigation, Writing – original draft. **Sarttrawut Tulaphol:** Conceptualization, Validation, Formal analysis, Writing – review & editing, Visualization. **Md Anwar Hossain:** Methodology, Investigation, Writing – original draft. **Clint N. Evrard:** Investigation. **Lee M. Thompson:** Conceptualization, Validation, Writing – review & editing, Supervision. **Noppadon Sathitsuksanoh:** Conceptualization, Methodology, Validation, Visualization, Supervision, Writing – review & editing, Funding acquisition.

Declaration of Competing Interest

The authors declare that they have no known competing financial interests or personal relationships that could have appeared to influence the work reported in this paper.

Acknowledgment

This material is based upon work supported by the National Science Foundation under Cooperative Agreement No. 1355438 and Internal Research Grant, Office of the Executive Vice President for Research, University of Louisville. This work was performed in part at the Conn Center for Renewable Energy Research at the University of Louisville, which belongs to the National Science Foundation NNCI KY Manufacturing and Nano Integration Node, supported by ECCS-1542174. The authors would like to thank Drs. Howard Fried and Panupon Khumsupan for their valuable comments and suggestions on the manuscript.

Supplementary materials

Supplementary material associated with this article can be found, in the online version, at doi:10.1016/j.mcat.2021.111848.

References

[1] A. Elgowainy, J. Han, H. Cai, M. Wang, G.S. Forman, V.B. DiVita, Environ. Sci. Technol. 48 (2014) 7612–7624.
[2] E. Regnier, Energy Econ 29 (2007) 405–427.
[3] O.B. Awodumi, A.O. Adewuyi, Energy Strategy Rev 27 (2020), 100434.
[4] M.C.Y. Chang, Curr. Opin. Chem. Biol. 11 (2007) 677–684.
[5] I. Delidovich, P. Hausoul, L. Deng, R. Pfützenreuter, M. Rose, R. Palkovits, Chem. Rev. 116 (2016) 1540–1599.
[6] L. Wu, T. Moteki, A. Gokhale, D. Flaherty, F.D. Toste, Chem, 1 (2016) 32–58.
[7] S. Chundawat, G. Beckham, M. Himmel, B. Dale, Annu. Rev. Chem. Biomol. Eng. 2 (2011) 121–145.
[8] A. Corma, S. Iborra, A. Velty, Chem. Rev. 107 (2007) 2411–2502.
[9] C. Zúñiga, M.S. Larrechi, G. Lligadas, J.C. Ronda, M. Galià, V. Cádiz, J. Polym. Sci., Part A: Polym. Chem. 49 (2011) 1219–1227.
[10] R.P. Fischer, G.R. Hartranft, J.S. Heckles, J. Appl. Polym. Sci. 10 (1966) 245–252.
[11] R. Zhang, J.A. Moore, Macromol. Symp. 199 (2003) 375–390.
[12] Z. Ping, W. Linbo, L. Bo-Geng, Polym. Degrad. Stab. 94 (2009) 1261–1266.
[13] F. Chu, C.J. Hawker, P.J. Pomery, D.J.T. Hill, J. Polym. Sci., Part A: Polym. Chem. 35 (1997) 1627–1633.
[14] K.H. Kim, J.Y. Moon, D.H. Ha, D.W. Park, React. Kinet. Catal. Lett. 75 (2002) 385–395.
[15] D.W. Park, D.H. Ha, J.Y. Park, J.Y. Moon, H.S. Lee, React. Kinet. Catal. Lett. 72 (2001) 219–227.
[16] A. Maiorana, S. Spinella, R.A. Gross, Biomacromolecules 16 (2015) 1021–1031.
[17] J. Ronda, G. Lligadas, M. Galia, V. Cadiz, React. Funct. Polym. 73 (2013) 381–395.
[18] J.A. Moore, T.J. Tannahill, High Perform. Polym. 13 (2001) S305–S316.
[19] J.J. Bozell, L. Moens, D.C. Elliott, Y. Wang, G.G. Neuenscwander, S.W. Fitzpatrick, R.J. Bilski, J.L. Jarnefeld, Resour. Conserv. Recycl., 28 (2000) 227–239.
[20] J.J. Bozell, G.R. Petersen, Green Chem 12 (2010) 539–554.
[21] Y.Q. Huang, C.K.C. Wong, J.S. Zheng, H. Bouwman, R. Barra, B. Wahlström, L. Neretin, M.H. Wong, Environ. Int. 42 (2012) 91–99.
[22] M. Janvier, L. Hollande, A.S. Jaufurally, M. Pernes, R. Ménard, M. Grimaldi, J. Beaugrand, P. Balaguer, P.H. Ducrot, F. Allais, ChemSusChem 10 (2017) 738–746.
[23] R. Machtinger, C.M.H. Combelles, S.A. Missmer, K.F. Correia, P. Williams, R. Hauser, C. Racowsky, Hum. Reprod. 28 (2013) 2735–2745.
[24] C.D. Kinch, K. Ibhazehiebo, J. Jeong, H.R. Habibi, D.M. Kurrasch, PNAS 112 (2015) 1475–1480.
[25] N. Lubick, Environ. Health Perspect. 118 (2010) A116.
[26] H. Gao, B. Yang, N. Li, L. Feng, X. Shi, W. Zhao, S. Liu, Medicine 94 (2015).
[27] Y. Guo, K. Li, X. Yu, J.H. Clark, Appl. Catal., B 81 (2008) 182–191.
[28] Q. Bu, H. Lei, A.H. Zacher, L. Wang, S. Ren, J. Liang, Y. Wei, Y. Liu, J. Tang, Q. Zhang, Bioresour. Technol. 124 (2012) 470–477.
[29] C. Chang, P. Cen, X. Ma, Bioresour. Technol. 98 (2007) 1448–1453.
[30] H. Chen, B. Yu, S. Jin, Bioresour. Technol. 102 (2011) 3568–3570.
[31] B. Girisuta, L.P.B.M. Janssen, H.J. Heeres, Ind. Eng. Chem. Res. 46 (2007) 1696–1708.
[32] H.A. Wittcoff, B.G. Reuben, J.S. Plotkin, Industrial Organic Chemicals, John Wiley & Sons, 2012.
[33] S. Van de Vyver, S. Helsen, J. Geboers, F. Yu, J. Thomas, M. Smet, W. Dehaen, Y. Román-Leshkov, I. Hermans, B.F. Sels, ACS Catal 2 (2012) 2700–2704.
[34] H. Liu, F. Zeng, L. Deng, B. Liao, H. Pang, Q. Guo, Green Chem 15 (2013) 81–84.
[35] A.R. Bader, A.D. Kontowicz, JACS 76 (1954) 4465–4466.
[36] Y. Shen, J. Sun, B. Wang, F. Xu, R. Sun, Bioresources 9 (2014) 3264–3275.
[37] S. Van de Vyver, J. Geboers, S. Helsen, F. Yu, J. Thomas, M. Smet, W. Dehaen, B. F. Sels, Chem. Commun. 48 (2012) 3497–3499.
[38] Y. Shen, J. Sun, B. Wang, F. Xu, R. Sun, BioResources 9 (2014) 12.
[39] M.R. Horn, A. Singh, S. Alomari, S. Goberna-Ferrón, R. Benages-Vilau, N. Chodankar, N. Motta, K. Ostrikov, J. MacLeod, P. Sonar, P. Gomez-Romero, D. Dubal, Energy Environ. Sci., 14 (2021) 1652–1700.
[40] N.I. Gumerova, A. Rompel, Nat. Rev. Chem. 2 (2018) 0112.
[41] L.P. Kazanskij, V.I. Spitsyn, Dokl. Akad. Nauk SSSR 227 (1976) 140–143.
[42] M. Misono, Catal. Today 144 (2009) 285–291.
[43] J. Zhong, J. Perez-Ramirez, N. Yan, Green Chem 23 (2021) 18–36.
[44] W. Deng, Q. Zhang, Y. Wang, Dalton Trans 41 (2012) 9817–9831.
[45] X. Yu, Y. Guo, K. Li, X. Yang, L. Xu, Y. Guo, J. Hu, J. Mol. Catal. A: Chem. 290 (2008) 44–53.
[46] Y. Guo, K. Li, J.H. Clark, Green Chem 9 (2007) 839–841.
[47] Y. Guo, K. Li, X. Yu, J.H. Clark, Appl. Catal. B: Environ. 81 (2008) 182–191.
[48] T. Kraemer, H.H. Maurer, Chapter 8 Non-opioid analgesics, in: M.J. Bogusz (Ed.), Handbook of Analytical Separations, Ed., Elsevier Science B.V., 2008, pp. 319–356.
[49] P.B. Kyle, Chapter 7 - Toxicology: GCMS, in: H. Nair, W. Clarke (Eds.), Mass Spectrometry for the Clinical Laboratory, Eds., Academic Press, San Diego, 2017, pp. 131–163.
[50] A. Shareef, M.J. Angove, J.D. Wells, J. Chromatogr. A 1108 (2006) 121–128.
[51] B. Jurado-Sánchez, E. Ballesteros, M. Gallego, Talanta 93 (2012) 224–232.
[52] S. Kinani, S. Bouchonnet, S. Bourcier, J.-M. Porcher, S. Aït-Aïssa, J. Chromatogr. A 1190 (2008) 307–315.

[53] K.R. Kim, M.K. Hahn, A. Zlatkis, E.C. Horning, B.S. Middleditch, J. Chromatogr. A 468 (1989) 289–301.
[54] J.A. Dias, J.P. Osegovic, R.S. Drago, J. Catal. 183 (1999) 83–90.
[55] R.S. Drago, J.A. Dias, T.O. Maier, JACS 119 (1997) 7702–7710.
[56] S. Van de Vyver, J. Geboers, S. Helsen, F. Yu, J. Thomas, M. Smet, W. Dehaen, B. Sels, Chem. Comm., 48 (2012) 3497–3499.
[57] H.-F. Liu, F.-X. Zeng, L. Deng, B. Liao, H. Pang, Q.-X. Guo, Green Chem 15 (2013) 81–84.
[58] R.K. Zeidan, V. Dufaud, M.E. Davis, J. Catal. 239 (2006) 299–306.
[59] S. Hunter, P. Savage, J. Org. Chem. 69 (2004) 4724–4731.
[60] R. Baetzold, G. Somorjai, J. Catal. 45 (1976) 94–105.
[61] P. Atkins, J. de Paula, J. Keeler, Atkins' Physical Chemistry, 11th Editon, Oxford University Press, 2018.
[62] B. Li, Y. Chen, L. Li, J. Kan, S. He, B. Yang, S. Shen, S. Zhu, J. Mol. Catal. A: Chem. 415 (2016) 160–167.
[63] K. Li, J. Hu, W. Li, F. Ma, L. Xu, Y. Guo, J. Mater. Chem. 19 (2009) 8628–8638.
[64] X. Yu, Y. Guo, K. Li, X. Yang, L. Xu, Y. Guo, J. Hu, J. Mol. Catal. A: Chem. 290 (2008) 44–53.
[65] H.F. Liu, F.X. Zeng, L. Deng, B. Liao, H. Pang, Q.X. Guo, Green Chem 15 (2013) 81–84.